lncRNA TUG1 inhibits the cancer stem cell-like properties of temozolomide-resistant glioma cells by interacting with EZH2

YIQIANG CAO[1], WENYING CHAI[2], YONGGANG WANG[1], DANG TANG[1],
DONGCHUAN SHAO[1], HAI SONG[1] and JIANG LONG[1]

[1]Department of Neurosurgery, First People's Hospital of Kunming; [2]Department of Breast Surgery,
The First Affiliated Hospital of Kunming Medical University, Kunming, Yunnan 650032, P.R. China

Abstract. Temozolomide (TMZ) is currently one of the first-line drugs used for the treatment of high-grade gliomas. However, TMZ resistance results in unsatisfactory therapeutic effects in gliomas. Cancer stem cells (CSCs) have recently been determined to serve a pivotal regulatory role in tumor metastasis, recurrence and chemoresistance. In addition, numerous reports have shown that long non-coding RNAs (lncRNAs) exert an essential role in the occurrence and development of tumors, and can be used as biomarkers for tumor diagnosis and treatment. Among them, studies have revealed that taurine upregulated gene 1 (TUG1) exhibits an important regulatory effect on the malignant biological behavior of glioma cells. Moreover, it has been reported that enhancer of Zeste homolog 2 polycomb repressive complex subunit 2 (EZH2) promotes tumorigenesis, including in glioma. However, the underlying mechanism of the interaction of TUG1 and EZH2 with CSCs of glioma remains elusive, and thus requires further clarification. The present study aimed to explore the role of TUG1 and EZH2 in TMZ resistance in glioma. Cell Counting Kit-8, colony formation, sphere formation and Annexin V-FITC/PI assays were used to detect the proliferation, clone formation efficiency, stemness and apoptosis of TMZ-resistant glioma cells. Xenograft tumor assay was used to detect the effect of TUG1 on the tumorigenesis of TMZ-resistant glioma cells. The present findings demonstrated that TUG1 exhibited a low expression in glioma cells, while EZH2 expression was the opposite. Moreover, it was observed that A172/TMZ cells possessed higher CSCs-like properties compared with parent cells, and that TUG1 and EZH2 were abnormally expressed in A172/TMZ cells. Knockdown of TUG1 or overexpression of EZH2 promoted A172/TMZ cell proliferation and CSCs-like properties, as well as inhibited their apoptosis, thereby enhancing the TMZ resistance of A172/TMZ cells. Furthermore, it was found that TUG1 alleviated the TMZ resistance of A172/TMZ cells by inhibiting EZH2 expression. Of note, overexpression of TUG1 inhibited the tumorigenicity of A172/TMZ cells by downregulating EZH2 expression *in vivo*. Collectively, the present study demonstrated that TUG1 served an essential regulatory role in TMZ resistance of gliomas.

Introduction

Glioma is the most prevalent histological subtype among primary tumors of the central nervous system that originates from normal glial cells (1). Glioma has been estimated to account for ~75% of brain malignant tumors worldwide (2). According to the 2016 World Health Organization classification, gliomas are generally classified into astrocytoma, oligodendroglioma, oligoastrocytoma, ependymoma and neuronal and mixed neuronal-glial tumors (3). Currently, the most definitive treatment modality for glioma is surgical resection of the primary lesion coupled with postoperative radiotherapy and chemotherapy (4). However, due to the limitations of brain function and structure, and the formation of chemical resistance of tumor cells, the recurrence rate after surgery is extremely high, resulting in a 5-year survival rate that is <5% (5).

Cancer stem cells (CSCs) have been confirmed to serve an significant regulatory role in tumor metastasis, recurrence and chemoresistance (6), and thus, they may represent a highly valuable therapeutic target in anti-cancer treatment. A study by Auffinger *et al* (7) revealed that temozolomide (TMZ)-treated glioma cells can interconvert from non-CSCs to CSCs, thereby supplementing the original tumor population, and ultimately enhancing its infiltration and TMZ resistance. More importantly, it has been suggested that it is of profound significance to investigate the molecular mechanism of alleviating the chemoresistance caused by CSCs of gliomas.

Long non-coding (lnc)RNAs are a large and functionally diverse class of non-RNA with a length of >200 nucleotides, which serve a crucial role in multiple diseases, such as tumors (8), kidney diseases (9) and cardiovascular diseases (10). Moreover, several studies have reported that the

Correspondence to: Dr Jiang Long, Department of Neurosurgery, First People's Hospital of Kunming, 504 Qingnian Road, Kunming, Yunnan 650032, P.R. China
E-mail: longjiang68@163.com

abnormal expression of lncRNA is closely associated with the occurrence and development of malignant tumors, including glioma (11-13). For instance, taurine upregulated gene 1 (TUG1) acts as a tumor-suppress factor of human glioma by promoting cell apoptosis (14). Interestingly, Zhao *et al* (15) discovered that TUG1 acted as a tumor-promoting factor for human glioma by promoting cell proliferation and invasion, and inhibiting its apoptosis. This indicates that TUG1 may be a tumor-promoting or a tumor suppressive factor in glioma under different circumstances. However, there is a lack of information regarding the mechanism of TUG1 regulating TMZ-resistance in CSCs of gliomas.

The histone-lysine N-methyltransferase, enhancer of Zeste homolog 2 polycomb repressive complex subunit 2 (EZH2), is an indispensable catalytic enzyme for the methylation of histone H3 lysine 27 (H3K27me) and histone H3 lysine 9 in mammalian cells (16). Furthermore, our previous studies reported that EZH2 acted as a cancer-promoting factor in glioma cells, and increased the proliferation, invasion and migration of glioma cells (17). However, the underlying mechanism of the interaction between TUG1 and EZH2 in the occurrence and development of glioma remains elusive.

Therefore, the present study aimed to investigate the underlying mechanism of TUG1 on the CSCs-like properties of TMZ-resistant glioma cells via EZH2. The purpose of this study was to provide basic experimental evidence and therapeutic targets for the treatment of glioma resistance.

Materials and methods

Cell lines and cell culture. For this study, normal human astrocytes (NHAs; NHA2; cat. no. CP-H122) were purchased from Procell Life Science & Technology Co., Ltd. Human glioblastoma cells (U251, TJ861, U87MG, T98G and A172; cat. nos. TCHu58, TCHu216, TCHu138, TCHu48 and TCHu171, respectively) were acquired from The Cell Bank of the Chinese Academy of Sciences. After short tandem repeat profiling, it was noted that U87MG cells were glioblastoma cells of unknown origin from the American Type Culture Collection. All cells were cultured in DMEM (Hyclone; Cytiva), supplemented with 10% FBS (Hyclone; Cytiva), 100 U/ml penicillin and 0.1 g/ml streptomycin, and were cultured in a 5% CO_2 incubator at 37°C for routine use.

To establish TMZ-resistant glioma cells, A172 cells were continuously exposed to 40-100 μM TMZ (Sigma-Aldrich; Merck KGaA) for 6 months daily (18). The expression level of drug resistance markers, glutathione S-transferase (GST)-π and P-glycoprotein 1 (P-gp), in A172 cells were assessed using western blot analysis. The obtained TMZ-resistant cells were named A172/TMZ cells.

Cell Counting Kit (CCK)-8 assay (Dojindo Molecular Technologies, Inc.) was used to evaluate the survival of A172/TMZ cells and the parent A172 cell line following treatment with TMZ (0, 5, 10, 20, 50, 100, 200, 500 and 1,000 μM). The IC_{50} calculator website (https://www.aatbio.com/tools/ic50-calculator) calculated the IC_{50} (50% inhibiting concentration) of TMZ in A172 cells and A172/TMZ cells. According to the IC_{50} obtained, the resistance index (RI) was further calculated using the following equation: IC_{50} of the drug-resistant cell/IC_{50} of the parent cell.

Construction and cell transfection. The cDNA strands of TUG1 and EZH2 were synthesized and purified by Shanghai GeneChem Co., Ltd. and were cloned into the expression vector pCDNA3.1 (Shanghai GeneChem Co., Ltd.). Moreover, the short hairpin RNA (shRNA/sh) of TUG1 and EZH2 was obtained from Shanghai GeneChem Co., Ltd. and was used to prepare the plasmid vector for transfection using a DNA Midiprep kit (Thermo Fisher Scientific, Inc.). Next, A172/TMZ cells treated with IC_{50} TMZ (450 μM) were transfected with the plasmid construct [40 nM sh-TUG1/EZH2 or sh-negative control (NC), 2 μg pcDNA3.1-TUG1/EZH2 vector or pcDNA3.1-NC empty vector] using Lipofectamine® 2000 reagent (Thermo Fisher Scientific, Inc.), following the manufacturer's instructions at 37°C for 24 h. Further experimentation was performed after cells were incubated at 37°C for 48 h. The shRNA sequences are as follows: sh-TUG1, 5'-CAGAAGAAT GGTACAAATCCAAG-3'; sh-EZH2, 5'-CTGATGAAGTAA AGAGTATGTTT-3'; and sh-NC, 5'-TTCTCCGAACGTGTC ACGTTT-3'.

Reverse transcription-quantitative (RT-q)PCR assay. Total RNA from NHAs and human glioma cell lines was extracted using TRIzol® reagent (Invitrogen; Thermo Fisher Scientific, Inc.), according to the manufacturer's protocol. Then, the concentration and purity of total RNA were determined using the UV absorption method. According to the QuantiTect RT kit (Qiagen, Inc.) instructions, 1 μg RNA was reverse transcribed into cDNA. Subsequently, GAPDH was employed as an internal control to detect the expression levels of TUG1 and EZH2 mRNA, as per the instructions of Power SYBR Green (Takara Biotechnology Co., Ltd.). The following thermocycling conditions were used for the qPCR: Initial denaturation at 95°C for 30 sec; followed by 40 cycles of 95°C for 3 sec and 60°C for 30 sec. Relative expression levels of each sample were calculated using the $2^{-\Delta\Delta Cq}$ method (19). The PCR primers for TUG1, EZH2 and GAPDH were as follows: TUG1 forward, 5'-AGCGTGGGTGTACGTAAAGG-3' and reverse, 5'-CCA AGGATTGGGGAACTGCT-3'; EZH2 forward, 5'-GGACTC AGAAGGCAGTGGAG-3' and reverse, 5'-CTTGAGCTG TCTCAGTCGCA-3'; and GAPDH forward, 5'-GCAACTAGG ATGGTGTGGCT-3' and reverse, 5'-TCCCATTCCCCAGCT CTCATA-3'.

Western blotting. After collecting the transfected cells, RIPA lysate (Beyotime Institute of Biotechnology) was used to extract the total protein in the cells, and a Bio-Rad protein (Bio-Rad Laboratories, Inc.) assay kit was used to determine the concentration and purity of the total protein. Then, 20 μg protein lysates were loaded onto 10% SDS-PAGE gels for electrophoresis, and separated proteins were subsequently transferred onto PVDF membranes. After blocking with 5% BSA [Roche Diagnostics (Shanghai) Co., Ltd.] at room temperature for 1 h, the membranes were incubated overnight at 4°C with primary antibodies against: EZH2 (1:1,000; cat. no. ab228697), GST-π (1:1,000; cat. no. ab138491), P-gp (1:1,000; cat. no. ab242104), Oct4 (1:1,000; cat. no. ab109183), Nanog (1:500; cat. no. ab173368) and SOX2 (1:1,000; cat. no. ab171380) (all from Abcam). Subsequently, membranes were washed three time with 0.1% TBS-Tween-20, 10 min each time, and further incubated with a secondary antibody

goat anti-mouse IgG H&L (1:5,000; cat. no. ab97019; Abcam) or goat anti-rabbit IgG H&L (1:2,000; cat. no. ab6721; Abcam) at room temperature for 2 h. After visualization using an ECL kit (Thermo Fisher Scientific, Inc.), the images were captured with an E-Gel Imager gel imager (Thermo Fisher Scientific, Inc.), while the gray value of the protein band was semi-quantified using ImageJ software (version 1.0; National Institutes of Health).

CCK-8 assay. A172 and A172/TMZ cells were seeded in a 96-well plate at a density of 5×10^3 cells/well and were incubated at 37°C for 24 h. According to the manufacturer's instructions, 10 μl CCK-8 solution was added to the medium at the indicated time intervals (0, 24, 48, 72 or 96 h), followed by incubation at 37°C for 2 h. Cells were subsequently detected using a microplate reader (Beckman Coulter, Inc.) at a wavelength of 450 nm.

Annexin V-FITC/PI assay. Cell apoptosis was detected using flow cytometry (FACSCalibur; BD Biosciences) using an Annexin V-FITC/PI kit (BD Biosciences). The apoptotic rate was calculated using the percentage of early + late apoptotic cells using CellQuest software (version 5.0; BD Biosciences). Briefly, A172/TMZ cells grown to log phase were collected, resuspended in pre-cooled PBS, centrifuged at 150 x g for 10 min at room temperature and washed. Following the addition of 300 μl 1X binding buffer to suspend the cells, 500 μl pre-cooling buffer and 5 μl Annexin V-FITC (BD Biosciences) were added and then incubated at room temperature for 15 min in the dark. Subsequently, 2.5 μl PI staining solution was added for 5 min in the dark at room temperature. Finally, 200 μl 1X binding buffer was added to each tube to detect cell apoptosis.

Colony formation assay. A172/TMZ cells were digested with 0.25% trypsin and suspended in DMEM. Then, cells were plated at a density of 500 cells/well, containing 10 ml DMEM, and incubated at room temperature for 2 weeks. When the clones were visible on the plate, the culture was stopped. Subsequently, the cells were fixed in 5 ml paraformaldehyde for 15 min and washed with PBS at room temperature. Then, the cells were stained with GIMSA staining solution for 20 min and then the staining solution was slowly washed off with PBS at room temperature. The number of cells was counted under a light microscope (Olympus Corporation; magnification, x100). The number of clones was counted using ImageJ software (version 1.0; National Institutes of Health), and >50 cells was considered a colony.

Sphere formation assay. A172/TMZ cells (70-90% confluence) were digested and centrifuged at 150 x g for 10 min at room temperature. Then, the medium was removed. After washing twice with PBS, the cells were resuspended in DMEM and counted. Cells were then seeded at a concentration of 1×10^4 cells/well into a 6-well plate for ultra-low adsorption cell culture, and were supplemented with 4 ml DMEM. After 10 days, the sphere state of cells was observed under a light microscope (Olympus Corporation; magnification, x100), and the number of sphere-forming cells was calculated by dividing the total number of spheres by the number of cells plated.

In vivo tumorigenicity. All experimental procedures involving animals were performed following the guidelines of the Animal Experimental Center of Kunming Medical University. Ethical approval was obtained from The First Affiliated Hospital of Kunming Medical University Ethics Committee (approval no. kmu-eac-2018056; date, 2018-05-01). For this experiment, 12 male nude mice (age, 6 weeks; weight, 20-30 g) were purchased from Shanghai Experimental Animal Center of the Chinese Academy of Sciences. All animal experiments in this study were conducted strictly adhering to the Guidelines for the Care and Use of Laboratory Animals proposed by the National Institutes of Health (20). The mice were housed in a specific pathogen-free environment at 22±2°C and 45-65% humidity, with a 12-h light/dark cycle and access to food and water *ad libitum*. Nude mice were subcutaneously injected with 2×10^5 A172/TMZ cells stably expressing TUG1 (pcDNA-lncRNA-TUG1) or the corresponding pcDNA3.1 NC vector. Then, 4 days after the injection, TMZ (10 mg/kg) was orally administered to mice. A total of 36 days after injection, mice of each group were euthanized by cervical dislocation. When tumors were palpable and visible, the tumor volume was measured weekly in two dimensions with a Vernier caliper and was calculated using the following formula: Length x width 2 x 0.5. All mice were sacrificed at 5 weeks following injection. At the end of the study, the tumors were isolated, weighed and imaged. Subsequently, the expression levels of Ki67, Bcl2 and Bax were examined via immunohistochemistry.

Immunohistochemistry. Tumor tissues were fixed with 10% paraformaldehyde at room temperature for 12 h, embedded in paraffin using an automatic Biological Tissue Embedding machine (Leica Microsystems, Inc.) and sliced into thin 4-μm thick sections. The sections were incubated with 3% H_2O_2 for 30 min at 37°C to block endogenous peroxidase activity and with 10% goat serum for 30 min at 37°C to block non-specific binding. The sections were then incubated with Ki67 (1:200; cat. no. ab16667), Bcl-2 (1:250; cat. no. ab32124) and Bax (1:50; cat. no. ab81083) primary antibodies (all from Abcam) for 12 h at 4°C. Then, the sections were incubated with goat anti-rabbit IgG H&L (1:1,000; cat. no. ab6721; Abcam) for 30 min at 37°C. Sections were then stained with a DAB kit (Thermo Fisher Scientific, Inc.) for 2 min at room temperature. The results were observed under a light microscope (Olympus Corporation; magnification, x200). As previously described, the expression levels of EZH2, GST-π, P-gp, Oct4, Nanog and SOX2 were detected using western blotting.

Statistical analysis. All statistical analyses were performed using SPSS software (version 20.0; IBM Corp.), while GraphPad Prism 7 (GraphPad Software, Inc.) was used for drawing graphs. The comparison between the two groups was performed using an unpaired Student's t-test, whereas the comparison between multiple groups was evaluated using a one-way ANOVA followed by Tukey's post hoc test. Data are presented as the mean ± SD. $P < 0.05$ was considered to indicate a statistically significant difference. All experiments were replicated three times.

Results

Expression levels of TUG1 and EZH2 in glioma cell lines. The expression levels of TUG1 and EZH2 were detected in NHA2
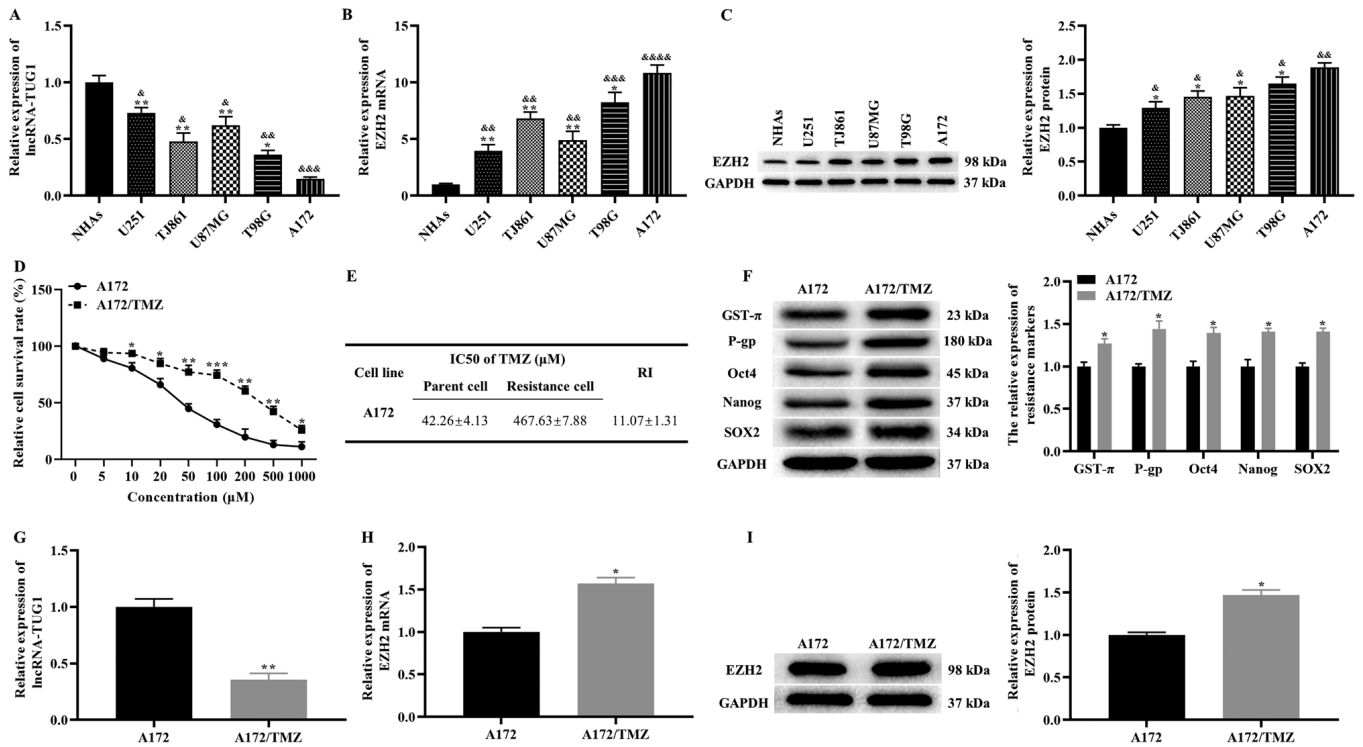
Figure 1. Expression levels of TUG1 and EZH2 in glioma cell lines and A172/TMZ cells. (A) Expression levels of TUG1 in each glioma cells line. (B) mRNA and (C) protein expression levels of EZH2 in each glioma cell line. (D) Cell Counting Kit-8 results showing the proliferation of A172/TMZ and A172 cells at different concentrations of TMZ. (E) IC_{50} and RI values of A172/TMZ and A172 cells. (F) Expression levels of drug resistance markers and cancer stem cell markers in A172/TMZ and A172 cells. (G) Expression levels of TUG1 in A172/TMZ and A172 cells. (H) mRNA and (I) protein expression levels of EZH2 in A172/TMZ and A172 cells. The error bars represent the mean ± SD of at least triplicate experiments. $^{\&}P<0.05$, $^{\&\&}P<0.01$, $^{\&\&\&}P<0.001$, $^{\&\&\&\&}P<0.0001$ vs. NHAs; $^{*}P<0.05$, $^{**}P<0.01$, $^{***}P<0.001$ vs. A172 cells. TMZ, temozolomide; TUG1, taurine upregulated gene 1; EZH2, enhancer of Zeste homolog 2 polycomb repressive complex subunit 2.

cells and glioma cell lines (U251, TJ861, U87MG, T98G and A172). Compared with NHA2 cells, TUG1 was downregulated in glioma cell lines (lowest in A172 cells), while the mRNA expression level of EZH2 exhibited the opposite pattern, based on RT-qPCR results (Fig. 1A and B). In addition, the western blotting results demonstrated that the protein expression level of EZH2 was significantly higher in glioma cell lines (highest in A172 cells) compared with that in NHA2 cells (Fig. 1C). Taken together, these results suggest that abnormal expression of TUG1 and EZH2 in glioma cell lines may be closely associated with the occurrence and development of glioma. Moreover, A172 cells were selected for further experiments.

Expression levels of TUG1 and EZH2 in A172/TMZ cells. Previous studies have reported that CSCs are closely associated with the TMZ resistance of tumor cells (21,22). Thus, A172/TMZ cells were established using increasing TMZ concentrations. The CCK-8 results revealed that the inhibitory effect of TMZ on the proliferation of A172/TMZ and A172 cells was dose-dependent (Fig. 1D). The IC_{50} and RI values of A172/TMZ cells were 467.63±7.88 and 11.07±1.31, respectively (Fig. 1E). Moreover, the expression levels of drug resistance markers, GST-π and P-gp, were detected. The western blotting results demonstrated that the expression levels of GST-π and P-gp were significantly higher in A172/TMZ cells compared with those in A172 cells (Fig. 1F). This finding suggests that the drug resistance level of A172/TMZ cells met the requirements of resistant strains.

Subsequently, the expression levels of CSCs markers, including Oct4, Nanog and SOX2, were measured in A172/TMZ and A172 cells. As expected, the expression levels of Oct4, Nanog and SOX2 were markedly higher in A172/TMZ cells compared with those in A172 cells (Fig. 1F). Thus, it was noted that A172/TMZ cells exhibited CSCs-like phenotypes.

The difference in TUG1 and EZH2 expression in the parent A172 cells was subsequently measured. The findings of RT-qPCR and western blotting demonstrated that the expression level of TUG1 was significantly lower in A172/TMZ cells compared with that in A172 cells, while opposite results were found for the mRNA and protein expression levels of EZH2 (Fig. 1G-I). Collectively, these results suggested that A172/TMZ cells displayed CSCs-like properties, and that TUG1 and EZH2 contributed to these properties.

Effects of the knockdown of TUG1 on the proliferation, apoptosis and CSCs-like properties of A172/TMZ cells. To analyze the effect of the knockdown of TUG1 on A172/TMZ cell survival and CSC-like properties, A172/TMZ cells were treated with 450 μM TMZ. The RT-qPCR results indicated that after knockdown of TUG1, the expression levels of TUG1 in A172/TMZ cells were significantly downregulated (Fig. 2A). Additionally, the results of CCK-8 revealed that the proliferative activity of A172/TMZ cells in the sh-lncRNA-TUG1 group was markedly higher compared with that in the sh-NC group (Fig. 2B).
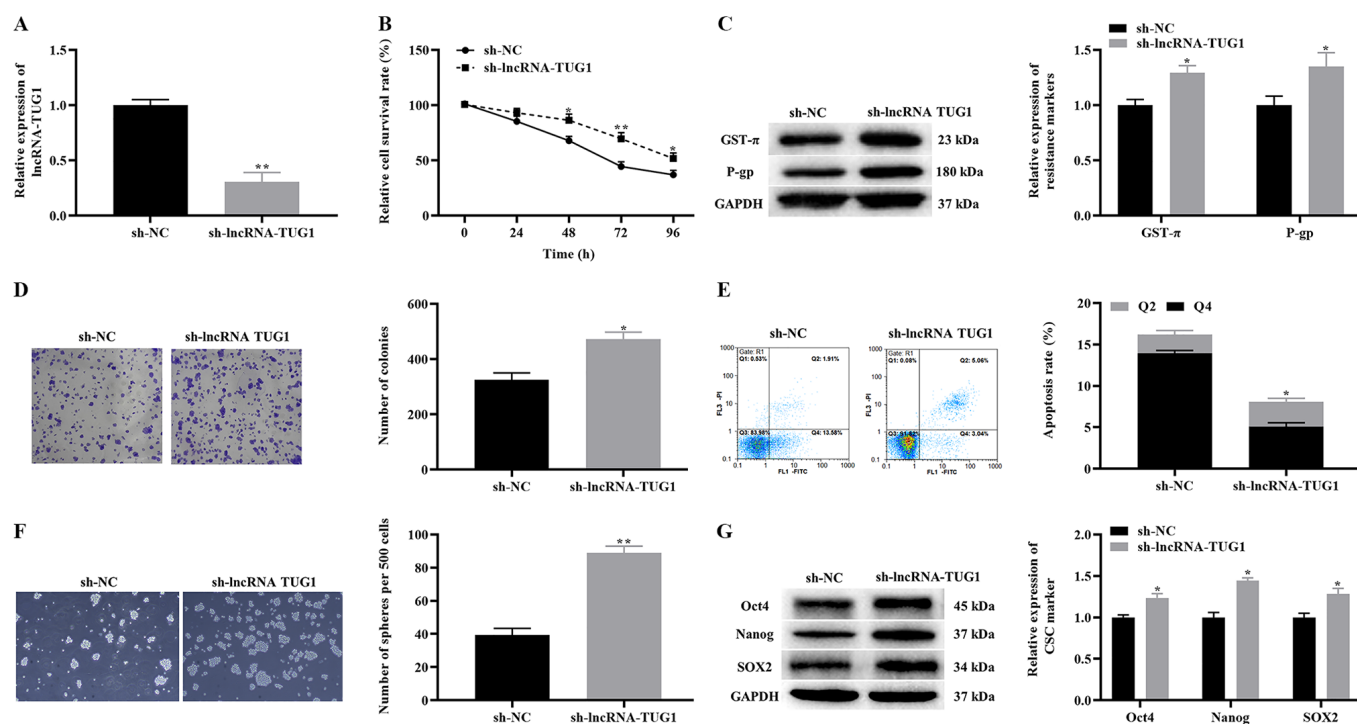
Figure 2. Effect of TUG1 knockdown on the proliferation, apoptosis and CSCs-like properties of A172/TMZ cells. (A) Effect of knockdown of TUG1 on the expression levels of TUG1 in A172/TMZ cells. (B) Cell Counting Kit-8 results of the proliferation of A172/TMZ cells before and after knockdown of TUG1. (C) Effects of TUG1 knockdown on the expression levels of drug resistance markers. (D) Clone formation results showing the proliferation of A172/TMZ cells in each group (magnification, x100). (E) Annexin V FITC/PI apoptosis depicting the apoptotic rates of A172/TMZ cells in each group. (F) Stem cell spheroidization experiment showing the spheroidizing ability of A172/TMZ cells (magnification, x100). (G) Western blotting results demonstrated the effect of TUG1 knockdown on the expression levels of CSCs markers. The error bars represent the mean ± SD of at least triplicate experiments. $^*P<0.05$, $^{**}P<0.01$ vs. sh-NC group. sh, short hairpin RNA; NC, negative control; lncRNA, long non-coding RNA; TMZ, temozolomide; TUG1, taurine upregulated gene 1; GST-π, glutathione S-transferase-π; P-gp, P-glycoprotein 1.

The effect of the knockdown of TUG1 on drug resistance markers was determined in A172/TMZ cells. The results demonstrated that knockdown of TUG1 could significantly upregulate the expression levels of GST-π and P-gp (Fig. 2C). Moreover, the proliferation of A172/TMZ cells was examined using the clone formation experiment, and the findings indicated that the proliferative activity of A172/TMZ cells was significantly higher in the sh-lncRNA-TUG1 group compared with that of the sh-NC group (Fig. 2D). It was also observed that the apoptosis level of A172/TMZ cells was lower in the sh-lncRNA-TUG1 group compared with that of the sh-NC group, according to the annexin V FITC/PI apoptosis experiment (Fig. 2E).

Next, the effect of the knockdown of TUG1 on the CSC-like properties of A172/TMZ cells was investigated. The results of the stem cell spheroidization experiment showed that, compared with the sh-NC group, the number of stem cells formed was increased in the sh-lncRNA-TUG1 group (Fig. 2F). The western blotting results revealed that, compared with the sh-NC group, the expression levels of Oct4, Nanog and SOX2 were significantly upregulated in the sh-lncRNA-TUG1 group (Fig. 2G). Based on these findings, it was identified that knockdown of TUG1 promoted the proliferation and CSC-like properties of A172/TMZ cells treated with TMZ, thereby inhibiting their apoptosis. As a result, enhancing the TMZ resistance of A172/TMZ cells.

Effects of the knockdown of EZH2 on the proliferation, apoptosis and CSCs-like properties of A172/TMZ cells. To test

the effect of the knockdown of EZH2 on the proliferation, apoptosis and CSC-like properties of A172/TMZ cells, A172/TMZ cells were treated with 450 μM TMZ. The western blotting results demonstrated that knockdown of EZH2 significantly downregulated the expression level of EZH2 in A172/TMZ cells (Fig. 3A). Then, CCK-8 and clone formation experiments were used to examine the effects of EZH2 knockdown on the proliferation of A172/TMZ cells. The findings indicated that compared with the sh-NC group, the proliferation activity and the number of cell clones of A172/TMZ cells were significantly lower in the sh-EZH2 group (Fig. 3B and D).

Subsequently, the expression levels of drug resistance markers were detected in A172/TMZ cells using western blotting. The results suggested that knockdown of EZH2 significantly downregulated GST-π and P-gp expression in A172/TMZ cells (Fig. 3C). It was demonstrated that knockdown of EZH2 can enhance the sensitivity of A172/TMZ cells to TMZ. Moreover, the Annexin V FITC/PI apoptosis experiment revealed that knockdown of EZH2 significantly increased the apoptotic rate of A172/TMZ cells (Fig. 3E). On the other hand, the findings of stem cell spheroidization experiments and western blotting demonstrated that knockdown of EZH2 significantly decreased the number of sphere-forming A172/TMZ cells and downregulated the expression levels of Oct4, Nanog, and SOX2 (Fig. 3F and G). In summary, these results suggested that knockdown of EZH2 inhibited the proliferation and CSC-like properties of A172/TMZ cells, as well as induced their apoptosis, thereby alleviating the TMZ resistance of A172/TMZ cells.
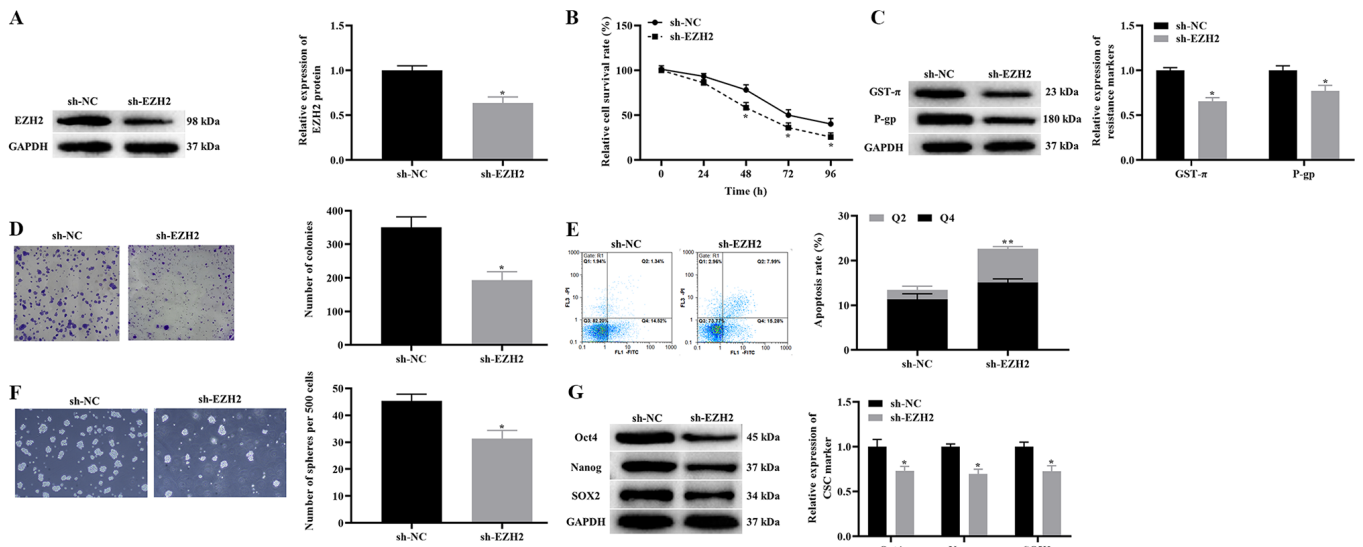
Figure 3. Effect of TUG1 knockdown on the proliferation, apoptosis and CSCs-like properties of A172/TMZ cells. (A) Western blotting detected the change of EZH2 expression in A172/TMZ cells after knockdown of EZH2. (B) Cell Counting Kit-8 results displaying the effect of the knockdown of EZH2 on the proliferation of A172/TMZ cells. (C) Western blotting results indicated the effect of EZH2 knockdown on the expression levels of drug resistance markers. (D) Clone formation experiment detected the effect of EZH2 knockdown on the clone formation of A172/TMZ cells (magnification, x100). (E) Annexin V FITC/PI apoptosis experiment displaying the effect of EZH2 knockdown on the apoptosis of A172/TMZ cells. (F) Stem cell spheroidization depicting the effect of EZH2 knockdown on the spheroidization ability of A172/TMZ cells (magnification, x100). (G) Western blotting results indicating the effect of EZH2 knockdown on the expression levels of CSCs markers. The error bars represent the mean ± SD of at least triplicate experiments. *P<0.05, **P<0.01 vs. sh-NC group. sh, short hairpin RNA; NC, negative control; TMZ, temozolomide; GST-π, glutathione S-transferase-π; P-gp, P-glycoprotein 1; EZH2, enhancer of Zeste homolog 2 polycomb repressive complex subunit 2.

Effects of TUG1 on the proliferation, apoptosis and CSCs-like properties of A172/TMZ cells via EZH2. Next, it was examined whether TUG1 may regulate the proliferation, apoptosis and CSC-like properties of A172/TMZ cells via EZH2. pcDNA-EZH2 and pcDNA-EZH2 + pcDNA-lncRNA-TUG1 were transfected into A172/TMZ cells. Then, A172/TMZ cells were treated with 450 µM TMZ. The western blotting results revealed that overexpression of EZH2 significantly upregulated the expression level of EZH2, while overexpression of EZH2 and TUG1 at the same time had no significant effect on the expression level of EZH2 compared with the control group (Fig. 4A). The results of CCK-8 and clone formation experiments indicated that, compared with the control group, the proliferation and colony number of A172/TMZ cells was significantly increased in the pcDNA-EZH2 group, while that in the pcDNA-EZH2 + pcDNA-lncRNA-TUG1 group showed no significant change (Fig. 4B and D).

Subsequently, the current study determined the expression levels of drug resistance markers. The results demonstrated that overexpression of EZH2 significantly upregulated the expression levels of GST-π and P-gp, while there was no significant difference in these proteins between the control and pcDNA-EZH2 + pcDNA-lncRNA-TUG1 groups (Fig. 4C). The annexin V FITC/PI apoptosis experiment results demonstrated that, compared with the control group, the apoptotic rate of A172/TMZ cells was decreased in the pcDNA-EZH2 group, while that in the pcDNA-EZH2 + pcDNA-lncRNA-TUG1 group showed no significant change (Fig. 4E). In addition, the results of western blotting and stem cell spheroidization experiments identified that overexpression of EZH2 significantly increased the expression levels of Oct4, Nanog and SOX2, as well as the spheroidizing ability of A172/TMZ

cells, while there was no significant difference between the control and pcDNA-EZH2 + pcDNA-lncRNA-TUG1 groups (Fig. 4F and G). Notably, compared with the pcDNA-EZH2 group, the expressions of EZH2, GST-π, P-gp, Oct4, Nanog and SOX2 were significantly downregulated (Fig. 4A, C and G), the proliferation, and number of colonies and spheres were significantly reduced (Fig. 4B, D and F) and the apoptosis rate was significantly increased (Fig. 4E) in the pcDNA-EZH2 + pcDNA-lncRNA-TUG1 group. Taken together, it was concluded that TUG1 inhibited the proliferation and CSC-like properties of A172/TMZ cells and induced apoptosis by downregulating the expression level of EZH2, thereby enhancing the TMZ sensitivity of A172/TMZ cells.

Effect of the overexpression of TUG1 on the tumorigenicity of A172/TMZ cells. To evaluate the effect of the overexpression of TUG1 on the tumorigenicity of A172/TMZ cells *in vivo*, nude mouse xenografts of A172/TMZ cells were constructed. The experimental mice were divided into two groups, where one group was injected with A172/TMZ cells transfected with pcDNA control, while the other group was injected with A172/TMZ cells transfected with pcDNA-TUG1. The RT-qPCR results demonstrated that the overexpression of TUG1 significantly increased the expression level of TUG1 of A172/TMZ cells (Fig. 5A), and the same results was observed in mice tumor tissue (Fig. 5B). The two nude mouse groups and tumor bodies are presented in Fig. 5C. We also recorded the volume and weight of the tumor. The data indicated that overexpression of TUG1 significantly reduced the volume and weight of the tumor, while exhibiting no effect on the body weight of the nude mice (Fig. 5D-F).
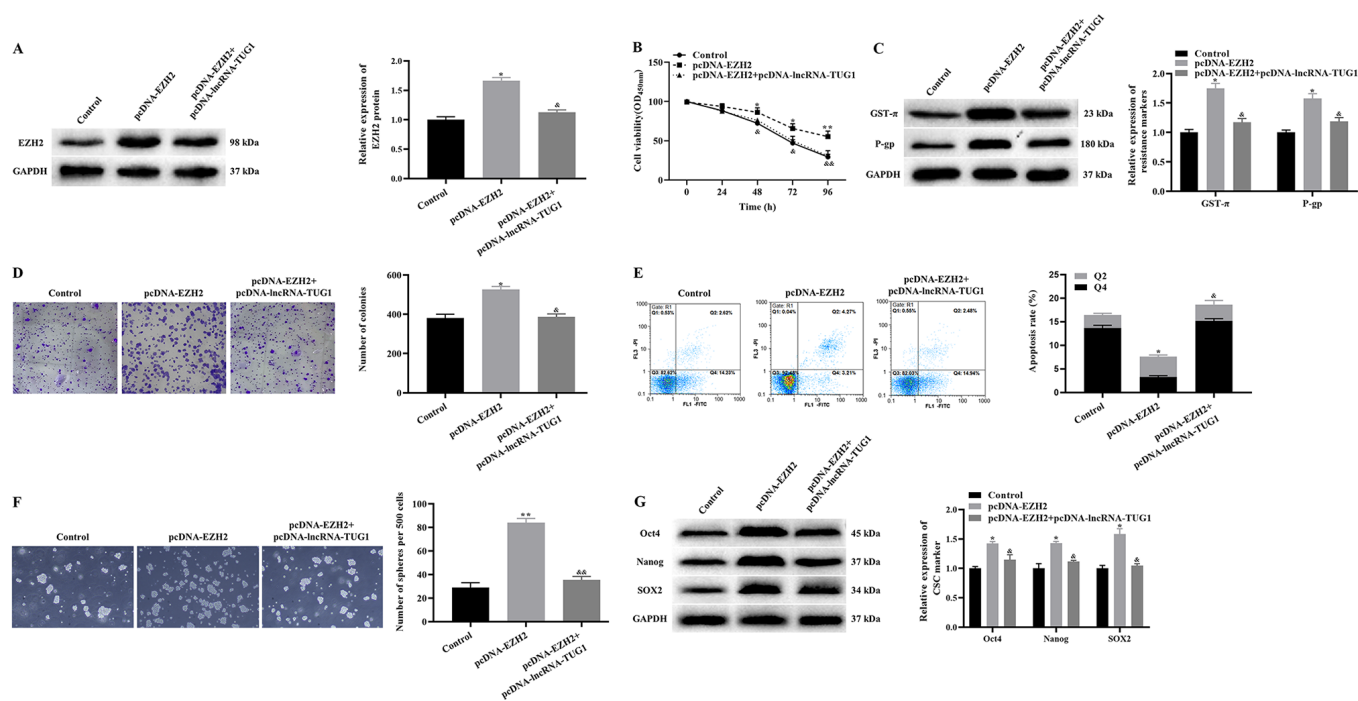
Figure 4. Effect of TUG1 on proliferation, apoptosis and CSC-like properties A172/TMZ cells via EZH2. (A) Western blotting results showing the transfection efficiency of pcDNA-EZH2. (B) Cell Counting Kit-8 results indicating the effect of the TUG1/EZH2 axis on the proliferation of A172/TMZ cells. (C) Expression levels of drug resistance markers. (D) Clone formation results indicating the effect of the TUG1/EZH2 axis on the proliferation of A172/TMZ cells (magnification, x100). (E) Annexin V FITC/PI apoptosis assay showing the effect of the TUG1/EZH2 axis on apoptosis of A172/TMZ cells. (F) Stem cell spheroidization test displaying the effect of the TUG1/EZH2 axis on the spheroidizing ability of A172/TMZ cells (magnification, x100). (G) Expression levels of CSCs markers. The error bars represent the mean ± SD of at least triplicate experiments. $^*P<0.05$, $^{**}P<0.01$ vs. Control group; $^&P<0.05$, $^{&&}P<0.01$ vs. pcDNA-EZH2 group. TMZ, temozolomide; GST-π, glutathione S-transferase-π; P-gp, P-glycoprotein 1; EZH2, enhancer of Zeste homolog 2 polycomb repressive complex subunit 2.

Next, the markers of proliferation and apoptosis were detected in tumors using immunohistochemistry. It was identified that the overexpression of TUG1 notably downregulated the expression levels of Ki67 and Bcl2, as well as upregulated the expression levels of Bax (Fig. 5G). Similarly, the western blotting results demonstrated that overexpression of TUG1 significantly downregulated the expression levels of EZH2, resistance markers (GST-π and P-gp) and CSCs markers (Oct4, Nanog and SOX2) (Fig. 5H). Based on the aforementioned findings, it was suggested that overexpression of TUG1 can inhibit the tumorigenicity of A172/TMZ cells.

Discussion

At present, TMZ is the first-choice drug for the treatment of glioma. However, patients with gliomas show poor prognosis due to the TMZ resistance of gliomas, and thus require aggressive treatment (23). Previous studies have reported that only <10% of patients survive for >5 years after treatment (24-26). The mechanism of glioma resistance has been attributed to the fact that chemical drugs targeting glioma cells exhibit a poor effect on CSCs, which results in chemotherapy-resistant CSCs driving more aggressive recurrent tumors (27). Another plausible explanation is that glioma cells can transform from non-CSCs to CSCs after chemotherapy, and subsequently, the phenotypic plasticity of this tumor cell population can lead to tumor regrowth (7,22). To the best of our knowledge, the present study demonstrated for the first time that TUG1 inhibited the CSCs-like properties

of TMZ-resistant glioma cells via EZH2, thereby alleviating TMZ resistance of gliomas.

TUG1 is a lncRNA located on chromosome 22q12, which was initially found to be involved the formation of photoreceptors by serving a key role in retinal development (28). The essential role of TUG1 in the occurrence and development of various malignant tumors, including glioma, has recently been confirmed. For example, Long et al (29) discovered that TUG1 was highly expressed in melanoma, where it upregulated the expression level of astrocyte elevated gene-1 protein by competitively binding miR-129-5p, which promoted the proliferation and invasion of melanoma cells, as well as inhibiting their apoptosis. Moreover, a study by Liao et al (30) reported that TUG1 was significantly downregulated in gliomas, and its overexpression could inhibit the proliferation of glioma cells, along with their apoptosis. Interestingly, several studies have highlighted that TUG1 can be utilized as a new therapeutic target for glioma, whereas its downregulation may inhibit cell proliferation and invasion, and promote the apoptosis of glioma U251 cells (15,31,32). However, the findings of Liao are inconsistent with the current results.

The present study identified that TUG1 had a tumor suppressor effect in gliomas, which was achieved by inhibiting CSCs-like properties. Currently, the associated mechanism of TUG1 with CSCs-like properties has been rarely studied. Nevertheless, there are recent multiple reports that have emphasized that TUG1 was involved in the regulation of drug resistance of a variety of malignant tumors. For example, TUG1 has been noted to be markedly
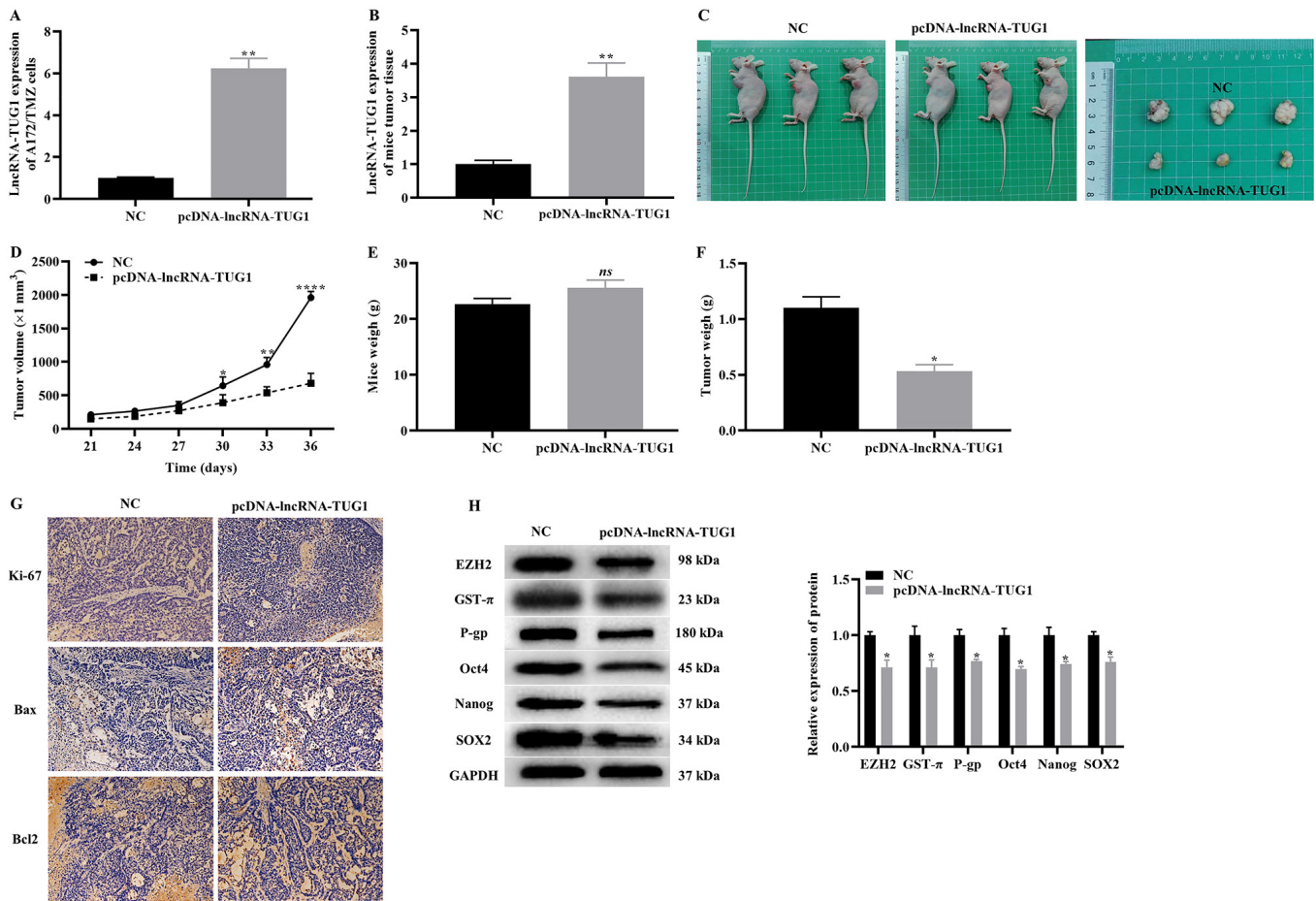
Figure 5. Effect of overexpression TUG1 on the tumorigenicity of A172/TMZ cells. Reverse transcription-quantitative PCR indicating (A) the transfection efficiency of pcDNA-TUG1 in A172/TMZ cells and (B) in mice tumor tissue. (C) Images of two groups nude mice and tumors. Changes in (D) tumor volume, (E) tumor mass and (F) body weight in the two groups of nude mice. (G) Immunohistochemistry detected the expression levels of cell proliferation and apoptosis markers. Original magnification, x200. (H) Western blotting results displaying the expression levels of EZH2, markers of drug resistance and CSCs. The error bars represent the mean ± SD of at least triplicate experiments. $^{*}P<0.05$, $^{**}P<0.01$ and $^{****}P<0.0001$ vs. NC group. NC, negative control group; lncRNA, long non-coding RNA; TMZ, temozolomide; TUG1, taurine upregulated gene 1; GST-π, glutathione S-transferase-π; P-gp, P-glycoprotein 1; EZH2, enhancer of Zeste homolog 2 polycomb repressive complex subunit 2.

downregulated in triple-negative breast cancer (TNBC), and at the same time it inhibits Wnt signaling pathway activation by regulating the miR-197/nemo like kinase molecular axis, thereby increasing the chemosensitivity of TNBC cells (33). Moreover, Xie *et al* (34) have shown that TUG1 inhibited the resistance of bladder urothelial carcinoma to adriamycin via the Wnt/β-catenin pathway. Some studies have also concluded that the Wnt signaling transcription factors, T-cell factor 1 and lymphoid enhancer binding factor 1, are upregulated in malignant astrocytic tumors (35). These reports suggest that TUG1 may also regulate the drug resistance of gliomas via the Wnt pathway. This may be the direction of future research.

Accumulating evidence has revealed that EZH2 is involved in the abnormal transcriptome of cancer cells (36). In addition, it has been established that EZH2, together with its enzymatic production of H3K27, are closely associated with poor prognosis in a variety of malignant tumors, such as prostate and breast cancer (37,38). Likewise, our previous studies reported that EZH2 promoted the malignant biological behavior of glioma cells. Moreover, EZH2 is involved in regulating the chemical resistance of various malignant tumors and the stemness of CSCs. It has been shown that EZH2 is upregulated in

glioma and glioma CSCs (39-41). Furthermore, inhibiting both BMI1 and EZH2 enhances the chemotherapy sensitivity of glioma stem cells (42). It has also been shown that phosphorylation of EZH2 activates STAT3 signaling by methylating STAT3, and promotes the tumorigenicity of glioblastoma CSC-like cells (43). Moreover, the direct transcriptional regulation of c-myc by EZH2 may constitute a novel mechanism underlying glioma CSC maintenance (44), which suggests that EZH2 may be a valuable new therapeutic target for glioma management. The present study demonstrated that EZH2 could promote CSCs-like properties to enhance the TMZ resistance of A172/TMZ cells.

Epigenetic disorders may induce tumorigenesis and influence targeted therapy (45) Carcinogenic pathways converge to the epigenome to maintain tumorigenesis, and so, epigenetic regulators may be particularly effective targets for cancer treatment (46). As a chromatin-modifying enzyme, EZH2 serves a vital role in the epigenetic silencing of genes via a complex mechanism (47). Most studies have demonstrated that 40% of gliomas harbor mutations in epigenetic regulatory factors, such as EZH2 (48-50). DNA methylation is a chemical modification of DNA, catalyzed by the DNA methyltransferase (DNMT)

enzyme, which serves a valuable role in epigenetic modifications. In particular, the polycomb group protein EZH2 directly controls DNA methylation (51), as EZH2 interacts with DNMTs to methylate the EZH2-binding promoter (50,52,53), which indicates that EZH2 is closely associated with the regulation of gene expression via epigenetic transcription. In the current study, EZH2 is likely to be involved in epigenetic regulation, but the specific mechanism requires further investigation.

In conclusion, the present study demonstrated that TUG1 inhibited CSCs-like properties and tumorigenicity, as well as induced the apoptosis of A172/TMZ cells by downregulating the expression level of EZH2, thereby alleviating the TMZ resistance of A172/TMZ cells.

Acknowledgements

Funding

Availability of data and materials

The datasets used and/or analyzed during the current study are available from the corresponding author on reasonable request.

Authors' contributions

JL and YC were responsible for the conceptualization and methodology; WC and YW performed the cell experiments, data analysis and prepared the figure; HS, DT and DS were responsible for animal experiments, data acquisition and data validation; JL and YC prepared the original draft of the manuscript, and reviewed and edited the manuscript. All authors confirm the authenticity of all raw data. All authors read and approved the final manuscript.

Ethics approval and consent to participate

Ethical approval was obtained from The First Affiliated Hospital of Kunming Medical University Ethics Committee (approval no. kmu-eac-2018056; date, 2018-05-01).

Patient consent for publication

Not applicable.

Competing interests

The authors declare that they have no competing interests.

References

1. Modrek AS, Bayin NS and Placantonakis DG: Brain stem cells as the cell of origin in glioma. World J Stem Cells 6: 43-52, 2014.
2. Lapointe S, Perry A and Butowski NA: Primary brain tumours in adults. Lancet 392: 432-446, 2018.
3. Wesseling P and Capper D: WHO 2016 Classification of gliomas. Neuropathol Appl Neurobiol 44: 139-150, 2018.
4. Alifieris C and Trafalis DT: Glioblastoma multiforme: Pathogenesis and treatment. Pharmacol Ther 152: 63-82, 2015.
5. Sun Q, Xu R, Xu H, Wang G, Shen X and Jiang H: Extracranial metastases of high-grade glioma: The clinical characteristics and mechanism. World J Surg Oncol 15: 181, 2017.
6. Chang JC: Cancer stem cells: Role in tumor growth, recurrence, metastasis, and treatment resistance. Medicine (Baltimore) 95 (Suppl 1): S20-S25, 2016.
7. Auffinger B, Tobias AL, Han Y, Lee G, Guo D, Dey M, Lesniak MS and Ahmed AU: Conversion of differentiated cancer cells into cancer stem-like cells in a glioblastoma model after primary chemotherapy. Cell Death Differ 21: 1119-1131, 2014.
8. Bhan A, Soleimani M and Mandal SS: Long noncoding RNA and cancer: A new paradigm. Cancer Res 77: 3965-3981, 2017.
9. Ignarski M, Islam R and Müller RU: Long non-coding RNAs in kidney disease. Int J Mol Sci 20: 3276, 2019.
10. Huang Y: The novel regulatory role of lncRNA-miRNA-mRNA axis in cardiovascular diseases. J Cell Mol Med 22: 5768-5775, 2018.
11. Buccarelli M, Lulli V, Giuliani A, Signore M, Martini M, D'Alessandris QG, Giannetti S, Novelli A, Ilari R, Giurato G, et al: Deregulated expression of the imprinted DLK1-DIO3 region in glioblastoma stemlike cells: Tumor suppressor role of lncRNA MEG3. Neuro Oncol 22: 1771-1784, 2020.
12. Lu C, Wei Y, Wang X, Zhang Z, Yin J, Li W, Chen L, Lyu X, Shi Z, Yan W and You Y: DNA-methylation-mediated activating of lncRNA SNHG12 promotes temozolomide resistance in glioblastoma. Mol Cancer 19: 28, 2020.
13. Voce DJ, Bernal GM, Wu L, Crawley CD, Zhang W, Mansour NM, Cahill KE, Szymura SJ, Uppal A, Raleigh DR, et al: Temozolomide treatment induces lncRNA MALAT1 in an NF-κB and p53 codependent manner in glioblastoma. Cancer Res 79: 2536-2548, 2019.
14. Li J, Zhang M, An G and Ma Q: LncRNA TUG1 acts as a tumor suppressor in human glioma by promoting cell apoptosis. Exp Biol Med (Maywood) 241: 644-649, 2016.
15. Zhao Z, Wang B, Hao J, Man W, Chang Y, Ma S, Hu Y, Liu F and Yang J: Downregulation of the long non-coding RNA taurine-upregulated gene 1 inhibits glioma cell proliferation and invasion and promotes apoptosis. Oncol Lett 15: 4026-4032, 2018.
16. Margueron R and Reinberg D: The Polycomb complex PRC2 and its mark in life. Nature 469: 343-349, 2011.
17. Wang XP, Shan C, Deng XL, Li LY and Ma W: Long non-coding RNA PAR5 inhibits the proliferation and progression of glioma through interaction with EZH2. Oncol Rep 38: 3177-3186, 2017.
18. Krell A, Wolter M, Stojcheva N, Hertler C, Liesenberg F, Zapatka M, Weller M, Malzkorn B and Reifenberger G: MiR-16-5p is frequently down-regulated in astrocytic gliomas and modulates glioma cell proliferation, apoptosis and response to cytotoxic therapy. Neuropathol Appl Neurobiol 45: 441-458, 2019.
19. Livak KJ and Schmittgen TD: Analysis of relative gene expression data using real-time quantitative PCR and the 2(-Delta Delta C(T)) method. Methods 25: 402-408, 2001.
20. National Research C: Guide for the Care and Use of Laboratory Animals. 8th edition. The National Academies Press, Washington, DC, 2011.
21. Chumakova A and Lathia JD: Outlining involvement of stem cell program in regulation of O6-methylguanine DNA methyltransferase and development of temozolomide resistance in glioblastoma: An Editorial Highlight for 'Transcriptional control of O^6-methylguanine DNA methyltransferase expression and temozolomide resistance in glioblastoma' on page 780. J Neurochem 144: 688-690, 2018.
22. Safa AR, Saadatzadeh MR, Cohen-Gadol AA, Pollok KE and Bijangi-Vishehsaraei K: Glioblastoma stem cells (GSCs) epigenetic plasticity and interconversion between differentiated non-GSCs and GSCs. Genes Dis 2: 152-163, 2015.
23. Lee SY: Temozolomide resistance in glioblastoma multiforme. Genes Dis 3: 198-210, 2016.
24. Stupp R, Mason WP, van den Bent MJ, Weller M, Fisher B, Taphoorn MJ, Belanger K, Brandes AA, Marosi C, Bogdahn U, et al: Radiotherapy plus concomitant and adjuvant temozolomide for glioblastoma. N Engl J Med 352: 987-996, 2005.
25. Thakkar JP, Dolecek TA, Horbinski C, Ostrom QT, Lightner DD, Barnholtz-Sloan JS and Villano JL: Epidemiologic and molecular prognostic review of glioblastoma. Cancer Epidemiol Biomarkers Prev 23: 1985-1996, 2014.

26. Ostrom QT, Gittleman H, Xu J, Kromer C, Wolinsky Y, Kruchko C and Barnholtz-Sloan JS: CBTRUS statistical report: Primary brain and other central nervous system tumors diagnosed in the United States in 2009-2013. Neuro Oncol 18 (Suppl 5): v1-v75, 2016.
27. Lee G, Auffinger B, Guo D, Hasan T, Deheeger M, Tobias AL, Kim JY, Atashi F, Zhang L, Lesniak MS, et al: Dedifferentiation of glioma cells to glioma stem-like cells by therapeutic Stress-induced HIF signaling in the recurrent GBM model. Mol Cancer Ther 15: 3064-3076, 2016.
28. Young TL, Matsuda T and Cepko CL: The noncoding RNA taurine upregulated gene 1 is required for differentiation of the murine retina. Curr Biol 15: 501-512, 2005.
29. Long J, Menggen Q, Wuren Q, Shi Q and Pi X: Long noncoding RNA taurine-upregulated gene1 (TUG1) promotes tumor growth and metastasis through TUG1/Mir-129-5p/astrocyte-elevated gene-1 (AEG-1) axis in malignant melanoma. Med Sci Monit 24: 1547-1559, 2018.
30. Liao Y, Zhang B, Zhang T, Zhang Y and Wang F: LncRNA GATA6-AS promotes cancer cell proliferation and inhibits apoptosis in glioma by downregulating lncRNA TUG1. Cancer Biother Radiopharm 34: 660-665, 2019.
31. Katsushima K, Natsume A, Ohka F, Shinjo K, Hatanaka A, Ichimura N, Sato S, Takahashi S, Kimura H, Totoki Y, et al: Targeting the Notch-regulated non-coding RNA TUG1 for glioma treatment. Nat Commun 7: 13616, 2016.
32. Cai H, Liu X, Zheng J, Xue Y, Ma J, Li Z, Xi Z, Li Z, Bao M and Liu Y: Long non-coding RNA taurine upregulated 1 enhances tumor-induced angiogenesis through inhibiting microRNA-299 in human glioblastoma. Oncogene 36: 318-331, 2017.
33. Tang T, Cheng Y, She Q, Jiang Y, Chen Y, Yang W and Li Y: Long non-coding RNA TUG1 sponges miR-197 to enhance cisplatin sensitivity in triple negative breast cancer. Biomed Pharmacother 107: 338-346, 2018.
34. Xie D, Zhang H, Hu X and Shang C: Knockdown of long non-coding RNA Taurine Up-Regulated 1 inhibited doxorubicin resistance of bladder urothelial carcinoma via Wnt/β-catenin pathway. Oncotarget 8: 88689-88696, 2017.
35. Pećina-Šlaus N, Kafka A, Tomas D, Marković L, Okštajner PK, Sukser V and Krušlin B: Wnt signaling transcription factors TCF-1 and LEF-1 are upregulated in malignant astrocytic brain tumors. Histol Histopathol 29: 1557-1564, 2014.
36. Kim KH and Roberts CW: Targeting EZH2 in cancer. Nat Med 22: 128-134, 2016.
37. McCabe MT and Creasy CL: EZH2 as a potential target in cancer therapy. Epigenomics 6: 341-351, 2014.
38. Chase A and Cross NC: Aberrations of EZH2 in cancer. Clin Cancer Res 17: 2613-2618, 2011.
39. Orzan F, Pellegatta S, Poliani PL, Pisati F, Caldera V, Menghi F, Kapetis D, Marras C, Schiffer D and Finocchiaro G: Enhancer of Zeste 2 (EZH2) is up-regulated in malignant gliomas and in glioma stem-like cells. Neuropathol Appl Neurobiol 37: 381-394, 2011.
40. Xu H, Zhao G, Zhang Y, Jiang H, Wang W, Zhao D, Hong J, Yu H and Qi L: Mesenchymal stem cell-derived exosomal microRNA-133b suppresses glioma progression via Wnt/β-catenin signaling pathway by targeting EZH2. Stem Cell Res Ther 10: 381, 2019.
41. Han B, Meng X, Wu P, Li Z, Li S, Zhang Y, Zha C, Ye Q, Jiang C, Cai J and Jiang T: ATRX/EZH2 complex epigenetically regulates FADD/PARP1 axis, contributing to TMZ resistance in glioma. Theranostics 10: 3351-3365, 2020.
42. Jin X, Kim LJY, Wu Q, Wallace LC, Prager BC, Sanvoranart T, Gimple RC, Wang X, Mack SC, Miller TE, et al: Targeting glioma stem cells through combined BMI1 and EZH2 inhibition. Nat Med 23: 1352-1361, 2017.
43. Kim E, Kim M, Woo DH, Shin Y, Shin J, Chang N, Oh YT, Kim H, Rheey J, Nakano I, et al: Phosphorylation of EZH2 activates STAT3 signaling via STAT3 methylation and promotes tumorigenicity of glioblastoma stem-like cells. Cancer Cell 23: 839-852, 2013.
44. Suvà ML, Riggi N, Janiszewska M, Radovanovic I, Provero P, Stehle JC, Baumer K, Le Bitoux MA, Marino D, Cironi L, et al: EZH2 is essential for glioblastoma cancer stem cell maintenance. Cancer Res 69: 9211-9218, 2009.
45. Khani P, Nasri F, Khani Chamani F, Saeidi F, Sadri Nahand J, Tabibkhooei A and Mirzaei H: Genetic and epigenetic contribution to astrocytic gliomas pathogenesis. J Neurochem 148: 188-203, 2019.
46. Mazor T, Pankov A, Johnson BE, Hong C, Hamilton EG, Bell RJA, Smirnov IV, Reis GF, Phillips JJ, Barnes MJ, et al: DNA methylation and somatic mutations converge on the cell cycle and define similar evolutionary histories in brain tumors. Cancer Cell 28: 307-317, 2015.
47. Eich ML, Athar M, Ferguson JE III and Varambally S: EZH2-targeted therapies in cancer: Hype or a reality. Cancer Res 80: 5449-5458, 2020.
48. Brennan CW, Verhaak RG, McKenna A, Campos B, Noushmehr H, Salama SR, Zheng S, Chakravarty D, Sanborn JZ, Berman SH, et al: The somatic genomic landscape of glioblastoma. Cell 155: 462-477, 2013.
49. Bian EB, Li J, Xie YS, Zong G, Li J and Zhao B: LncRNAs: New players in gliomas, with special emphasis on the interaction of lncRNAs With EZH2. J Cell Physiol 230: 496-503, 2015.
50. Bian EB, Li J, He XJ, Zong G, Jiang T, Li J and Zhao B: Epigenetic modification in gliomas: Role of the histone methyltransferase EZH2. Expert Opin Ther Targets 18: 1197-1206, 2014.
51. Viré E, Brenner C, Deplus R, Blanchon L, Fraga M, Didelot C, Morey L, Van Eynde A, Bernard D, Vanderwinden JM, et al: The polycomb group protein EZH2 directly controls DNA methylation. Nature 439: 871-874, 2006.
52. Ning X, Shi Z, Liu X, Zhang A, Han L, Jiang K, Kang C and Zhang Q: DNMT1 and EZH2 mediated methylation silences the microRNA-200b/a/429 gene and promotes tumor progression. Cancer Lett 359: 198-205, 2015.
53. Wang R and Liu X: Epigenetic regulation of prostate cancer. Genes Dis 7: 606-613, 2019.